

Finite resolution measurement of the non-classical polarization statistics of entangled photon pairs

Holger F. Hofmann

Department of Physics, Faculty of Science, University of Tokyo

7-3-1 Hongo, Bunkyo-ku, Tokyo 113-0033, Japan

(February 1, 2008)

Abstract

By limiting the resolution of quantum measurements, the measurement induced changes of the quantum state can be reduced, permitting subsequent measurements of variables that do not commute with the initially measured property. It is then possible to experimentally determine correlations between non-commuting variables. The application of this method to the polarization statistics of entangled photon pairs reveals that negative conditional probabilities between non-orthogonal polarization components are responsible for the violation of Bell's inequalities. Such negative probabilities can also be observed in finite resolution measurements of the polarization of a single photon. The violation of Bell's inequalities therefore originates from local properties of the quantum statistics of single photon polarization.

I. INTRODUCTION

Perhaps the most convincing proof of the non-classical nature of quantum statistics is the violation of Bell's inequalities by a pair of entangled spin-1/2 particles [1]. Several experimental tests of these inequalities have been performed on pairs of entangled photons generated either by two photon emission [2,3] or by parametric down conversion [4,5]. These experimental tests compare the polarization correlations of photon pairs emitted at the same time for different sets of orthogonal polarizations. While no information about the relationship between non-orthogonal polarization directions of the single photon are revealed in such measurements, the statistics obtained correspond to the quantum theoretical prediction. Since the quantum formalism from which the violation of Bell's inequalities is derived is widely accepted, one might wonder whether it should not be possible to obtain a clearer understanding of the origin of this non-classical effect by investigating the unique statistical connection between non-commuting quantum variables in more detail. In particular, finite resolution measurements can provide quantitative information about a quantum variable without destroying the quantum coherence between different eigenstate components of that variable [6]. By applying finite resolution measurements, it is therefore possible to identify the non-classical correlations between non-commuting variables directly [7,8]. In the following, an experiment is proposed to determine the correlations between non-orthogonal polarizations of entangled photon pairs. It is shown that the violation of Bell's inequalities results from the negative joint probabilities arising from local non-classical correlations of the photon polarization. It is then possible to give a local interpretation of entanglement based on standard quantum mechanics.

The rest of the paper is organized as follows. In section II, the application of finite resolution measurements to the polarization of a single photon is discussed and fundamental non-classical correlations are derived. In section III, the experimental setup for a measurement of entangled photon pairs is presented and the statistical results of such a measurement are derived. In section IV, the non-classical features of the statistics are identified and the implications concerning the nature of entanglement are discussed. Finally, the conclusions are summarized in section V.

II. FINITE RESOLUTION MEASUREMENTS

A. The generalized measurement postulate

A measurement assigns a quantity to a system property based on the observable action of the system on some measurement device. The uncertainty principle of quantum mechanics requires that this interaction between the system and the measurement setup introduces noise into properties that do not commute with the measured variable. Therefore, the classical ideal of a complete determination of all system properties is unattainable. Nevertheless it is possible to obtain quantitative information on the correlations between non-commuting variables by limiting the measurement resolution. Such a finite resolution measurement is described by the generalized measurement operator $\hat{P}_{\hat{s}}(s_m)$, which assigns a continuous measurement value s_m to the operator \hat{s} [6]. It reads

$$\hat{P}_{\delta s}(s_m) = (2\pi\delta s^2)^{-\frac{1}{4}} \exp\left(-\frac{(s_m - \hat{s})^2}{4\delta s^2}\right). \quad (1)$$

For a given initial state $|\psi_{\text{in}}\rangle$, the probability $P(s_m)$ of obtaining a measurement result s_m and the state $|\psi_{\text{out}}\rangle$ after the measurement are then given by

$$\begin{aligned} P(s_m) &= \langle\psi_{\text{in}}| \hat{P}_{\delta s}^2(s_m) |\psi_{\text{in}}\rangle \\ |\psi_{\text{out}}\rangle &= \frac{1}{\sqrt{P(s_m)}} \hat{P}_{\delta s}(s_m) |\psi_{\text{in}}\rangle. \end{aligned} \quad (2)$$

Note that this generalized measurement postulate does not restrict the values of an operator variable to the eigenvalues of that operator. Eigenvalues emerge only in infinitely precise measurements. One of the fundamental problems in the discussion of quantum mechanics is that eigenvalues are often identified with “elements of reality” [9,10] regardless of the measurement context discussed. By assigning a continuous measurement value to the operator variable in a finite resolution measurement this identification is avoided, allowing a determination of quantitative results beyond the spectrum of its eigenvalues.

B. Finite resolution measurement of photon polarization

The polarization of a single photon can be described in terms of the Stokes parameters \hat{s}_i . In terms of the circular polarization eigenstates $|R\rangle$ and $|L\rangle$, the operators of the three single photon Stokes parameters may be written as

$$\begin{aligned} \hat{s}_1 &= |L\rangle\langle R| + |R\rangle\langle L| \\ \hat{s}_2 &= i|L\rangle\langle R| - i|R\rangle\langle L| \\ \hat{s}_3 &= |R\rangle\langle R| - |L\rangle\langle L|. \end{aligned} \quad (3)$$

\hat{s}_1 represents the intensity difference between the x and y polarizations, \hat{s}_2 represents the intensity difference between the polarizations along the diagonals between the x and y axes, and \hat{s}_3 represents the intensity difference between the circular polarizations. Since only one photon is considered, the eigenvalues of each Stokes parameter are ± 1 .

A finite resolution measurement of photon polarization can be realized by using a polarization sensitive beam displacer that shifts the x-polarization component relative to the y-polarization component of the light field. The displacement of the photon trajectory in the beam displacer can be interpreted as the action of the one-photon Stokes parameter \hat{s}_1 . The polarization of the photon is then described by a continuous value s_{1m} of the Stokes parameter \hat{s}_1 obtained from the measurement of the transversal photon position after the beam displacer. The measurement resolution depends on the ratio of the displacement and the width of the input beam. If the transversal profile of the light field is Gaussian, the generalized measurement postulate describes the single photon polarization statistics obtained by measuring the polarization dependent displacement of the photon. In terms of the circular polarization eigenstates, the measurement operator is given by

$$\begin{aligned}
\hat{P}_{\delta s}(s_{1m}) &= (2\pi\delta s^2)^{-\frac{1}{4}} \exp\left(-\frac{s_{1m}^2 + 1}{4\delta s^2}\right) \\
&\times \left(\cosh\left(\frac{s_{1m}}{2\delta s^2}\right) (|R\rangle\langle R| + |L\rangle\langle L|) \right. \\
&\left. + \sinh\left(\frac{s_{1m}}{2\delta s^2}\right) (|R\rangle\langle L| + |L\rangle\langle R|) \right). \tag{4}
\end{aligned}$$

This operator describes the changes in the quantum state of the single photon polarization conditioned by the finite resolution measurement of the Stokes parameter \hat{s}_1 .

C. Joint measurements of non-orthogonal polarizations

In order to measure the correlated non-orthogonal polarization components of a single photon, the finite resolution measurement can be combined with a fully resolved polarization measurement. By rotating the polarization by an angle of $\pi/4$ and separating the x and y components as shown in figure 1, the eigenvalues of the Stokes parameter \hat{s}_2 are measured. Two spatial patterns emerge, corresponding to the conditional distributions of continuous measurement results s_{1m} of the Stokes parameter \hat{s}_1 associated with a final measurement of the eigenvalues $+1$ or -1 of the Stokes parameter \hat{s}_2 . The positive valued operator measure (POM) describing the joint measurement of \hat{s}_1 and \hat{s}_2 is defined by projections onto the states

$$|s_{1m}; s_2 = \pm 1\rangle = \hat{P}_{\delta s}(s_{1m}) \frac{1}{\sqrt{2}} (|R\rangle \pm i|L\rangle). \tag{5}$$

The joint probabilities $P(s_{1m}; s_2 = \pm 1)$ for measuring a finite resolution value of s_{1m} for the Stokes parameter \hat{s}_1 followed by an eigenvalue of $s_2 = \pm 1$ for the Stokes parameter \hat{s}_2 is then given by

$$\begin{aligned}
P(s_{1m}; s_2 = \pm 1) &= |\langle s_{1m}; s_2 = \pm 1 | \psi_{\text{in}} \rangle|^2 \\
&= \frac{1}{2} \left| \langle R | \hat{P}_{\delta s}(s_{1m}) | \psi_{\text{in}} \rangle \mp i \langle L | \hat{P}_{\delta s}(s_{1m}) | \psi_{\text{in}} \rangle \right|^2, \tag{6}
\end{aligned}$$

where $|\psi_{\text{in}}\rangle$ is an arbitrary initial state. This POM thus assigns quantitative results to both Stokes parameters, allowing a derivation of correlations between the polarization components of a single photon.

If the light field entering the measurement setup shown in figure 1 is polarized along the diagonal between the x and y axes, the initial photon state is given by

$$|\psi_{\text{in}}\rangle = \frac{1}{\sqrt{2}} (|R\rangle + i|L\rangle). \tag{7}$$

The joint probabilities of the measurement results s_{1m} and s_2 can then be determined using equation (6). In its most compact form, it reads

$$\begin{aligned}
P(s_{1m}; s_2 = +1) &= (2\pi\delta s^2)^{-\frac{1}{2}} \exp\left(-\frac{s_{1m}^2 + 1}{2\delta s^2}\right) \cosh^2\left(\frac{s_{1m}}{2\delta s^2}\right) \\
P(s_{1m}; s_2 = -1) &= (2\pi\delta s^2)^{-\frac{1}{2}} \exp\left(-\frac{s_{1m}^2 + 1}{2\delta s^2}\right) \sinh^2\left(\frac{s_{1m}}{2\delta s^2}\right). \tag{8}
\end{aligned}$$

Note that $P(s_{1m} = 0; s_2 = -1)$ is always exactly equal to zero, even if δs is larger than one. Obviously, this result is too exact to be explained in terms of a random measurement error superimposed on classical statistics. The result for a measurement resolution of $\delta s = 0.6$ is illustrated in figure 2. The peaks in $P(s_{1m}; s_2 = -1)$ are shifted to values of about ± 1.1 and the asymmetry of the peaks seems to favor even higher values. These results can hardly be explained by statistics originating only from the eigenvalues of $s_1 = \pm 1$.

D. Negative conditional probabilities and non-classical correlations in the polarization of single photons

The non-classical features of the joint probabilities $P(s_{1m}; s_2 = \pm 1)$ can be analyzed by expressing the result as a sum of shifted normalized Gaussian distributions

$$G_{\delta s}(s_{1m} - d) := (2\pi\delta s^2)^{-\frac{1}{2}} \exp\left(-\frac{(s_{1m}^2 - d)^2}{2\delta s^2}\right). \quad (9)$$

In terms of these Gaussians, the joint probabilities read

$$\begin{aligned} P(s_{1m}; s_2 = +1) &= \frac{1}{4}G_{\delta s}(s_{1m} + 1) + \exp\left(-\frac{1}{2\delta s^2}\right)\frac{1}{2}G_{\delta s}(s_{1m}) + \frac{1}{4}G_{\delta s}(s_{1m} - 1) \\ P(s_{1m}; s_2 = -1) &= \frac{1}{4}G_{\delta s}(s_{1m} + 1) - \exp\left(-\frac{1}{2\delta s^2}\right)\frac{1}{2}G_{\delta s}(s_{1m}) + \frac{1}{4}G_{\delta s}(s_{1m} - 1). \end{aligned} \quad (10)$$

Each Gaussian contribution to the joint probabilities given in equation (10) can be identified with elements of the density matrix of the original state in the eigenstate basis of the observable \hat{s}_1 . As discussed in a previous paper [6], the measurement of s_{1m} modifies each matrix element by a decoherence factor given by the difference of the eigenvalues and an information factor depending on the difference between the measurement result s_{1m} and the average of the eigenvalues.

The decoherence factor $\exp(-1/(2\delta s^2))$ is a result of the quantum noise in the measurement required by the uncertainty principle. In the case of the beam displacer acting on single photons, it is the uncertainty of the wave vector dependent time the photon spends in the birefringent medium which randomly rotates the Stokes vector around the s_1 axis. Since this noisy interaction is statistically independent of the measurement result, it is possible to separate its effect from the information obtained about the system. A hypothetical noise free measurement then reveals negative probabilities of $s_2 = -1$ for measurement results s_{1m} close to zero [6]. These negative probabilities describe the non-classical correlations between non-commuting operator variables [7,8].

The information about \hat{s}_1 obtained in the measurement modifies the statistical weight of each density matrix element by a Gaussian function of the difference between the measurement result s_{1m} and the average of the two eigenvalues of the density matrix element. In particular, the Gaussians centered around $s_{1m} = 0$ represent contributions from the quantum coherence between the $s_1 = +1$ and the $s_1 = -1$ eigenstates conditioned by a measurement of s_{1m} . Measurement results close to $s_{1m} = 0$ enhance the coherence and increase the probability of $s_2 = +1$ to values above 1, while measurement results far away from $s_{1m} = 0$ reduce the coherence, lowering the probability of $s_2 = +1$ to values below 1. In order to explain

this non-classical correlation between s_1 and s_2 , some measure of reality must be attributed to $s_1 = 0$, even though it is not an eigenvalue of \hat{s}_1 [7]. Since the width of the Gaussians represents the effect of random noise in the readout of the finite resolution measurement, it is reasonable to identify each Gaussian contribution with its average value of s_{1m} . The continuum of measurement values s_{1m} can then be represented by a discrete set of three values at $s_1 = \pm 1$ and $s_1 = 0$. The joint probabilities for these three values of s_1 and the two eigenvalues of s_2 read

$$\begin{aligned} P(s_1 = -1; s_2 = -1) &= 1/4 & P(s_1 = -1; s_2 = +1) &= 1/4 \\ P(s_1 = 0; s_2 = -1) &= -1/2 & P(s_1 = 0; s_2 = +1) &= 1/2 \\ P(s_1 = +1; s_2 = -1) &= 1/4 & P(s_1 = +1; s_2 = +1) &= 1/4. \end{aligned} \quad (11)$$

These joint probabilities explain the non-classical features of the quantum statistics obtained from the single photon polarization measurement setup shown in figure 1 for any value of the measurement resolution δs .

It should be noted that the measurement setup itself defines an asymmetry between \hat{s}_1 and \hat{s}_2 since the non-eigenvalue of zero appears only in the statistics of the initial finite resolution measurement of \hat{s}_1 . This dependence on the order of measurement is reflected in the operator order dependence of quantum mechanical expectation values. In order to identify the operator properties responsible for the appearance of negative probabilities in the statistical properties, it is useful to characterize the measurement statistics in terms of the correlation between s_{1m}^2 and s_2 ,

$$\begin{aligned} C(s_{1m}^2, s_2) &= \langle s_{1m}^2 s_2 \rangle - \langle s_{1m}^2 \rangle \langle s_2 \rangle \\ &= -2(\langle s_{1m}^2 \rangle - \delta s^2) \langle s_2 \rangle \\ &= -2 \exp\left(-\frac{1}{2\delta s^2}\right), \end{aligned} \quad (12)$$

where $\langle \rangle$ denotes statistical averages over actual measurement results. This correlation may be expressed in terms of the operator expectation values of $|\psi_{\text{in}}\rangle$ as

$$C(s_1^2, s_2) = \exp\left(-\frac{1}{2\delta s^2}\right) \left(\langle \psi_{\text{in}} | \hat{s}_1 \hat{s}_2 \hat{s}_1 | \psi_{\text{in}} \rangle - \langle \psi_{\text{in}} | \hat{s}_1^2 | \psi_{\text{in}} \rangle \langle \psi_{\text{in}} | \hat{s}_2 | \psi_{\text{in}} \rangle \right). \quad (13)$$

As explained above, the exponential factor expresses the randomization of \hat{s}_2 induced by the measurement of \hat{s}_1 according to the uncertainty principle. For $\delta s \rightarrow \infty$, the noise introduced in the measurement of \hat{s}_1 goes to zero and the correlation is given by the operator expectation values of the initial state. Due to the operator ordering, the anti-correlation between s_1^2 and s_2 is an inherent statistical property of $|\psi_{\text{in}}\rangle$ even though $|\psi_{\text{in}}\rangle$ is an eigenstate of \hat{s}_2 . Thus operator ordering allows a correlation between fluctuating properties and seemingly well defined operator variables of the quantum state.

This property implies that even the eigenvalues of a quantum state do not represent “elements of reality”. Consequently, it is wrong to assign measurement values to physical properties before the measurement *even if the measurement result can be predicted with certainty*. Since the violation of Bell’s inequalities depends on the assignment of such “elements of reality” it is not surprising that it can be violated by quantum theory. In the following, it will be shown how the violation of Bell’s inequalities can be explained in terms of negative joint probabilities obtained from finite resolution measurements.

III. MEASUREMENT OF POLARIZATION ENTANGLEMENT

A. Entangled photons

Entangled photon pairs can be created in two photon emission [2,3] or in parametric down conversion [4,5]. The precise polarization statistics may vary depending on the geometry of the setup. In order to express the violation of Bell's inequalities in terms of the Stokes parameters \hat{s}_1 and \hat{s}_2 , it is useful to rotate the polarizations of the two photons in such a way that the quantum state is given by

$$|\psi_{a,b}\rangle = \frac{1}{\sqrt{2}} \left(|R;L\rangle + \exp\left(-i\frac{\pi}{4}\right) |L;R\rangle \right). \quad (14)$$

This state is an eigenstate of two polarization correlations,

$$\begin{aligned} \frac{1}{\sqrt{2}} (\hat{s}_1(a) + \hat{s}_2(a)) \hat{s}_1(b) |\psi_{a,b}\rangle &= |\psi_{a,b}\rangle \\ -\frac{1}{\sqrt{2}} (\hat{s}_1(a) - \hat{s}_2(a)) \hat{s}_2(b) |\psi_{a,b}\rangle &= |\psi_{a,b}\rangle. \end{aligned} \quad (15)$$

The sum of these two eigenvalues violates a Bell's inequality of the form

$$K = s_1(a)s_1(b) + s_2(a)s_1(b) - s_1(a)s_2(b) + s_2(a)s_2(b) \leq 2. \quad (16)$$

It is therefore not possible to interpret the polarization statistics by assigning eigenvalues of ± 1 to each Stokes parameter. However, as indicated by the results of finite resolution measurements on the polarization of single photons discussed in section II above, such an identification of physical properties with their eigenvalues is not even consistent with the correlated statistics of local single photon properties. The non-classical statistical properties responsible for the violation of Bell's inequality (16) can be derived in detail by applying the finite resolution measurement setup introduced above to realize a polarization measurement on the entangled photon pairs given by equation (14).

B. Experimental setup and measurement statistics

Figure 3 shows the experimental setup for a measurement of the correlations in the Bell's inequality (16). The detector arrays record coincidence counts between the right and left hand side. Each detector array corresponds to an eigenvalue measurement of \hat{s}_2 . The spatial coordinate at which the photon is registered corresponds to the continuous measurement value s_{1m} of \hat{s}_1 . Each measurement result can then be identified with a point in one of four two dimensional graphs. The probability distribution for the measurement outcomes of the joint measurements may be determined by projections onto the non-orthogonal, non-normalized set of states

$$|\mathbf{s}_{1m}(a); s_{1m}(b); s_2(a) = \pm 1; s_2(b) = \pm 1\rangle = \hat{P}_{\hat{s}_2}(s_{1m}(a)) \hat{P}_{\hat{s}_2}(s_{1m}(b)) \frac{1}{2} (|R;R\rangle + s_2(a)i|R;L\rangle + s_2(b)i|R;L\rangle - s_2(a)s_2(b)|L;L\rangle). \quad (17)$$

In their most compact form, the joint probabilities of the measurement results $s_{1m}(a)$, $s_{1m}(b)$, $s_2(a)$, and $s_2(b)$ for the entangled input state $|\psi(a, b)\rangle$ given by equation (14) read

$$\begin{aligned}
P(s_{1m}(a); s_{1m}(b); s_2(a) = \pm 1; s_2(b) = \pm 1) = & \\
& \frac{\sqrt{2}}{16\pi\delta s^2} \exp\left(-\frac{s_{1m}(a)^2 + s_{1m}(b)^2 + 2}{2\delta s^2}\right) \\
& \times \left(2 \sinh\left(\frac{s_{1m}(a)s_2(b) - s_{1m}(b)s_2(a)}{2\delta s^2}\right) \cosh\left(\frac{s_{1m}(a)s_2(b) + s_{1m}(b)s_2(a)}{2\delta s^2}\right)\right. \\
& + \left(\sqrt{2} + s_2(a)s_2(b)\right) \cosh^2\left(\frac{s_{1m}(a)s_2(b) + s_{1m}(b)s_2(a)}{2\delta s^2}\right) \\
& \left. + \left(\sqrt{2} - s_2(a)s_2(b)\right) \sinh^2\left(\frac{s_{1m}(a)s_2(b) - s_{1m}(b)s_2(a)}{2\delta s^2}\right)\right). \tag{18}
\end{aligned}$$

Figure 4 shows the results for a measurement resolution of $\delta s = 0.6$. At this intermediate resolution, quantum mechanical interference effects are especially visible [7]. In particular, separate peaks can be resolved clearly, but quantum interference effects are visible in the asymmetric peak shapes and in the zero probability valleys in the $s_{1m} \approx 0$ regions separating the peaks. As in the single photon case discussed in section II above, it is indeed possible to interpret these features entirely in terms of Gaussian distributions. However, negative probability contributions centered around values of $s_{1m} = 0$ have to be included in order to explain the asymmetries and the regions of extremely low probabilities near $s_{1m} = 0$ separating the peaks corresponding to quantized results around $s_{1m} = \pm 1$.

C. Violation of Bell's inequality by the finite resolution measurement statistics

As in the one photon case, the regions of low probability at values of $s_{1m}(a/b) = 0$ can be traced back to negative joint probabilities. The measurement probabilities given by equation (18) may be expressed as a sum of shifted normalized Gaussian distributions

$$G_{\delta s}(s_{1m}(a) - d_a; s_{1m}(b) - d_b) := (2\pi\delta s^2)^{-1} \exp\left(-\frac{(s_{1m}(a)^2 - d_a)^2 + (s_{1m}(b)^2 - d_b)^2}{2\delta s^2}\right). \tag{19}$$

Since the shifts d_a and d_b may be -1 , 0 or $+1$, respectively, each of the four sums has nine components associated with joint probabilities of the four Stokes parameters. The probability distribution of the measurement results is then given by the sum

$$\begin{aligned}
P(s_{1m}(a); s_{1m}(b); s_2(a) = \pm 1; s_2(b) = \pm 1) = & \\
& \frac{\sqrt{2} + 1}{16\sqrt{2}} (G_{\delta s}(s_{1m}(a) + 1; s_{1m}(b) + 1) + G_{\delta s}(s_{1m}(a) - 1; s_{1m}(b) - 1)) \\
& + \frac{\sqrt{2} - 1}{16\sqrt{2}} (G_{\delta s}(s_{1m}(a) + 1; s_{1m}(b) - 1) + G_{\delta s}(s_{1m}(a) - 1; s_{1m}(b) + 1)) \\
& + \exp\left(-\frac{1}{2\delta s^2}\right) \frac{1}{8\sqrt{2}} s_2(b) (G_{\delta s}(s_{1m}(a) + 1; s_{1m}(b)) - G_{\delta s}(s_{1m}(a) - 1; s_{1m}(b)))
\end{aligned}$$

$$\begin{aligned}
& - \exp\left(-\frac{1}{2\delta s^2}\right) \frac{1}{8\sqrt{2}} s_2(a) (G_{\delta s}(s_{1m}(a); s_{1m}(b) + 1) - G_{\delta s}(s_{1m}(a); s_{1m}(b) - 1)) \\
& + \exp\left(-\frac{1}{\delta s^2}\right) \frac{1}{4\sqrt{2}} s_2(a) s_2(b) G_{\delta s}(s_{1m}(a); s_{1m}(b)) .
\end{aligned} \tag{20}$$

Using this decomposition, it is a straightforward matter to determine the averages corresponding to the correlations of the Bell's inequality (16) by summing over $s_2(a)$ and $s_2(b)$ and integrating over the continuous results $s_{1m}(a)$ and $s_{1m}(b)$. The result reads

$$\langle K \rangle = \frac{1}{\sqrt{2}} \left(1 + \exp\left(-\frac{1}{2\delta s^2}\right) \right)^2. \tag{21}$$

This expectation value exceeds the maximal value of 2 allowed by inequality (16) for measurement resolutions of $\delta s > 1.143$. The violation of Bell's inequality can therefore be obtained directly from the measurement statistics for sufficiently low resolutions of the \hat{s}_1 measurements. An example for this direct violation of Bell's inequality is shown in figure 5 for a measurement resolution of $\delta s = 2$. At this low resolution, quantization effects are not resolved. The non-classical properties of the statistics are observable in the shift of the peak maxima for $s_2(a) = -s_2(b)$ to values greater than $s_{1m} = +1$ or lower than $s_{1m} = -1$. Specifically, the maximum probability density for $s_2(a) = +1$ and $s_2(b) = -1$ is at $s_{1m}(a) == s_{1m}(b) = 1.383$ and the maximum for $s_2(a) = -1$ and $s_2(b) = +1$ is at $s_{1m}(a) == s_{1m}(b) = -1.383$. The value of K at these points would be equal to 3.68.

While it might be tempting to interpret the statistics in terms of polarization components greater than $+1$ or smaller than -1 , the high resolution results of figure 4 and the analysis of single photon polarization in section II suggests that the true reason for the shifted peaks are negative probabilities around $s_{1m}(a) = s_{1m}(b) = 0$. In order to obtain a consistent interpretation of the measurement results for both high and low resolutions, it is necessary to identify the decoherence factor $\exp(1/(2\delta s^2))$ with the quantum noise induced reduction of the expectation values of $\hat{s}_2(a)$ and $\hat{s}_2(b)$. It is then possible to remove the effects of noise and of finite measurement resolution from the measurement statistics, tracing the violation of Bell's inequality directly to the appearance of negative probabilities in the joint probabilities for $s_1(a), s_2(a), s_1(b)$, and $s_2(b)$.

IV. DISENTANGLING ENTANGLEMENT: INTERPRETATION OF THE NON-CLASSICAL STATISTICS

A. Negative conditional probabilities in photon entanglement

As in the case of single photon polarization discussed in section II, the sum of Gaussians given in equation (20) can be interpreted in terms of joint probabilities for $s_1(a), s_2(a), s_1(b)$, and $s_2(b)$ by identifying the average of each Gaussian with the appropriate value of s_1 . The joint probabilities for all 36 combinations of the six contributions from $s_1(a)$ and $s_2(a)$ with the six contributions from $s_1(b)$ and $s_2(b)$ characterizing the statistics of the entangled state $|\psi_{a,b}\rangle$ are shown in table I. From these probabilities, the statistical weight of different contributions to the sum correlation K in inequality (16) can be determined.

The joint probabilities can be classified according to whether the values of $s_1(a)$ and $s_1(b)$ are zero or not. There are sixteen contributions with both $s_1(a)$ and $s_1(b)$ non-zero. These cases correspond to the classical expectation that the values of s_1 should be equal to the eigenvalues observed in high resolution measurements. Consequently, they are the only contributions that are not diminished by the decoherence factor for small δs . Moreover, their probabilities are all positive. In eight of these sixteen cases, three of the four correlations in inequality (16) are equal to +1 and one is equal to -1, for a total of $K = 2$. The reverse is true for the remaining eight cases, resulting in a total of $K = -2$ for the sum of correlations in inequality (16). The probability of each case is equal to $(2 + s_1(a)s_1(b)\sqrt{2})/32$. Summing up the probability of the eight cases with $K = 2$ thus results in a total probability of $(4 + \sqrt{2})/8$ or roughly 67.7 %. The eight cases with $K = -2$ have a total probability of $(4 - \sqrt{2})/8$, or 32.3 %. The average value of K for these “classical” contributions to the joint probability is therefore equal to $1/\sqrt{2}$, as evidenced by the limit of equation (21) for $\delta s \rightarrow 0$. Obviously, the violation of Bell’s inequality must originate from the remaining twenty contributions with at least one value of s_1 equal to zero.

There are sixteen contributions with one value of s_1 equal to zero and the other value non-zero. Two of the four correlations in the inequality (16) are then equal to zero, while the other two may be either plus or minus one each. In four cases, they are both equal to plus one ($K = 2$), in eight cases, they have opposite sign ($K = 0$), and in the remaining four cases, they are both equal to minus one ($K = -2$). The probabilities for these cases are $\pm\sqrt{2}/16$. As a result, the total probability for the four cases with $K = 2$ is equal to $\sqrt{2}/4$ or 35.4%, the total probabilities for the eight cases with $K = 0$ cancel to zero, and the total probability for $K = -2$ is $-\sqrt{2}/4$ or -35.4%. This negative probability more than outweighs the 32.3 % of the classical contributions, explaining the increase of the expectation value of K beyond the limit of 2. However, the effect is further enhanced by the contributions from $s_1(a) = s_1(b) = 0$.

There are four contributions with $s_1(a) = s_1(b) = 0$. Only the correlation $\langle s_2(a)s_2(b) \rangle$ is non-zero in these cases. Two cases have $K = 1$ and a positive probability of $\sqrt{2}/8$, and two cases have $K = -1$ and a negative probability of $-\sqrt{2}/8$. This adds a total probability of 35.4 % for $K = 1$ and -35.4 % for $K = -1$.

The probability distribution over values of K can be summarized as follows:

$$\begin{aligned} P(K = 2) &= 103.1\% & P(K = -2) &= -3.1\% \\ P(K = 1) &= 35.4\% & P(K = -1) &= -35.4\% \\ P(K = 0) &= 0\%. \end{aligned} \tag{22}$$

The high expectation value of K is a result of the negative probabilities for combinations of $s_1(a), s_2(a), s_1(b)$, and $s_2(b)$ with $K < 0$. In the measured probability distributions described by equations (18) and (20), these negative probabilities appear as a suppression of the probability for values of s_1 close to zero, pushing the peak of the probability distribution beyond the eigenvalue limit of ± 1 . Since s_{1m} is not restricted to eigenvalues of \hat{s}_1 , the contributions to the expectation value of K taken from the measured distribution (18) shown in figure 4 may exceed the classical limit. Even though a direct observation of the negative probabilities is of course impossible, the continuous distribution of finite resolution measurement results thus reveals clear evidence of these non-classical statistical features.

B. Quantum noise and negative probabilities in entangled systems

The negative conditional probabilities shown in table I allow an interpretation of the measurement statistics in terms of individual measurement results observed separately in branch a and in branch b . There is neither a need for action at a distance, nor for non-local properties. The non-classical feature required to explain the violation of Bell's inequalities is expressed in the negative probabilities which are possible even in individual quantum systems because the uncertainty principle does not allow an isolated measurement of a joint probability of non-commuting variables.

Once the relationship between uncertainty and negative conditional probabilities is understood, the problem of non-locality in entangled systems can be resolved by introducing local decompositions of the entangled state density matrix based on negative probability components of the local density matrices. For the state discussed above, one possible decomposition reads

$$|\psi_{a,b}\rangle\langle\psi_{a,b}| = \frac{1}{4}\hat{1}(a) \otimes \hat{1}(b) + \frac{1}{4\sqrt{2}}(\hat{s}_1(a) + \hat{s}_2(a)) \otimes \hat{s}_1(b) \\ + \frac{1}{4\sqrt{2}}(\hat{s}_1(a) - \hat{s}_2(a)) \otimes \hat{s}_2(b) - \frac{1}{4}\hat{s}_3(a) \otimes \hat{s}_3(b). \quad (23)$$

All by themselves, the Stokes parameter operators \hat{s}_i would not qualify as density matrices because of their negative eigenvalues. Once negative eigenvalue components are permitted, however, the decomposition given above can be interpreted as a separation of the entangled density matrix into products of local density matrices. The reason why density matrices with negative probability eigenvalues may be used in the decomposition of entangled states is that any measurement performed on system a mixes contributions to the density matrix of system b in such a way that the information required to isolate the negative conditional probabilities represented by the negative eigenvalues is lost.

Effectively, the uncertainty in system a necessarily “covers up” the negative eigenvalues of the density matrix components of system b by mixing them with positive components. Entanglement can therefore be explained by the local properties of quantum measurements described previously [6]. In the light of this result, it is not surprising that some applications of quantum mechanics such as quantum computation can work without entanglement [11,12]. The most fundamental property of quantum mechanics is not entanglement, but local non-classical correlations represented by the operator-ordering dependence of expectation values and the negative conditional probabilities obtained from finite resolution measurements.

V. CONCLUSIONS

The interpretation of quantum statistics cannot be based on the assumption that potential measurement results represent “elements of reality” whether the actual measurement is performed or not. This is not only true for entangled systems, but also for combinations of finite resolution measurements performed to obtain the correlations between non-commuting operator variables in a single quantum system. As a result, concepts such as photon polarization have to be reviewed critically in order to understand the relationship between eigenvalues and operator variables.

The experimental approach proposed above allows a direct determination of the non-classical features of the polarization statistics for both single photons and entangled pairs. Its application to the violation of Bell's inequalities reveals details of the statistical relationships between all four polarization components. A full set of conditional probabilities can be obtained from the statistics of a single measurement, revealing the negative conditional probabilities that are responsible for the violation of Bell's inequalities. A comparison with the single photon polarization statistics reveals that such negative probabilities are also observable in the polarization of a single photon. The property responsible for the violation of Bell's inequalities is therefore a local feature of quantum statistics. Once the implications of the operator formalism are accepted, entanglement can be understood as a special case of the non-classical features observable in local correlations.

ACKNOWLEDGMENT

The author would like to acknowledge support from the Japanese Society for the Promotion of Science, JSPS, and thank Dr. Takao Fuji for helpful discussions of the experimental aspects.

REFERENCES

- [1] J.S. Bell, Physics (Long Island City, N.Y.) **1**,195 (1964).
- [2] S.J. Freedman and J.F. Clauser, Phys. Rev. Lett. **28**, 938 (1972).
- [3] A. Aspect, J. Dalibard, and G. Roger, Phys. Rev. Lett. **49**, 1804 (1982).
- [4] Z.Y. Ou, L. Mandel, Phys. Rev. Lett. **61**, 50 (1988).
- [5] Y.H. Shih, C. Alley, Phys. Rev. Lett. **61**, 2921 (1988).
- [6] H.F. Hofmann, Phys. Rev. A **62**, 022103 (2000).
- [7] H.F. Hofmann, Phys. Rev. A **61**, 033815 (2000).
- [8] H.F. Hofmann, T. Kobayashi, and A. Furusawa, Phys. Rev. A **62**, 013806 (2000).
- [9] A. Einstein, B. Podolsky, and N. Rosen, Phys. Rev. **47**, 777 (1935).
- [10] N.D. Mermin, Phys. Today **43** (6), 9 (1990).
- [11] R. Fitzgerald, Physics Today **53**(1), 20(2000).
- [12] S.L. Braunstein, C.M. Caves, R. Jozsa, N. Linden, S.Popescu, and R. Schack, Phys. Rev. Lett. **83**, 1054 (1999).

FIGURES

FIG. 1. Schematic representation of the experimental setup for a joint measurement of non-orthogonal polarizations. The beam displacer separates the incoming light into two parallel beams. The polarization is then rotated by an angle of $\pi/4$ before the light beam is split at the polarizer. The overlapping transversal profile of the beams is illustrated at the detector arrays.

FIG. 2. Probability distribution $P(s_{1m}; s_2)$ for an initial eigenstate of $s_2 = +1$ at a resolution of $\delta s = 0.6$. Note the asymmetry and the shifted maxima obtained for $s_2 = -1$.

FIG. 3. Schematic representation of the experimental setup for a measurement of polarization correlations on entangled photons. The setup of the branches a and b are as shown in figure 1. Coincidence counts are registered in one of four channels as illustrated.

FIG. 4. Contour plot of the probability distribution $P(s_{1m}(a); s_{1m}(b); s_2(a); s_2(b))$ at a resolution of $\delta s = 0.6$. While the major peaks appear to be close to the eigenvalues at $s_{1m} = \pm 1$, the shape of the peaks and the separation between them reveals the same non-classical statistical effects seen in figure 2.

FIG. 5. Contour plot of the probability distribution $P(s_{1m}(a); s_{1m}(b); s_2(a); s_2(b))$ at a resolution of $\delta s = 2$. The peaks for $s_2(a) = -s_2(b)$ are at $s_{1m}(a) = s_{1m}(b) = \pm 1.383$. The contribution to the average value of K at these points is 3.68.

TABLES

TABLE I. Table of conditional probabilities derived from the results shown in figure 4. Note that the negative probabilities roughly coincide with regions of zero probability in the measurement statistics.

Figure 1

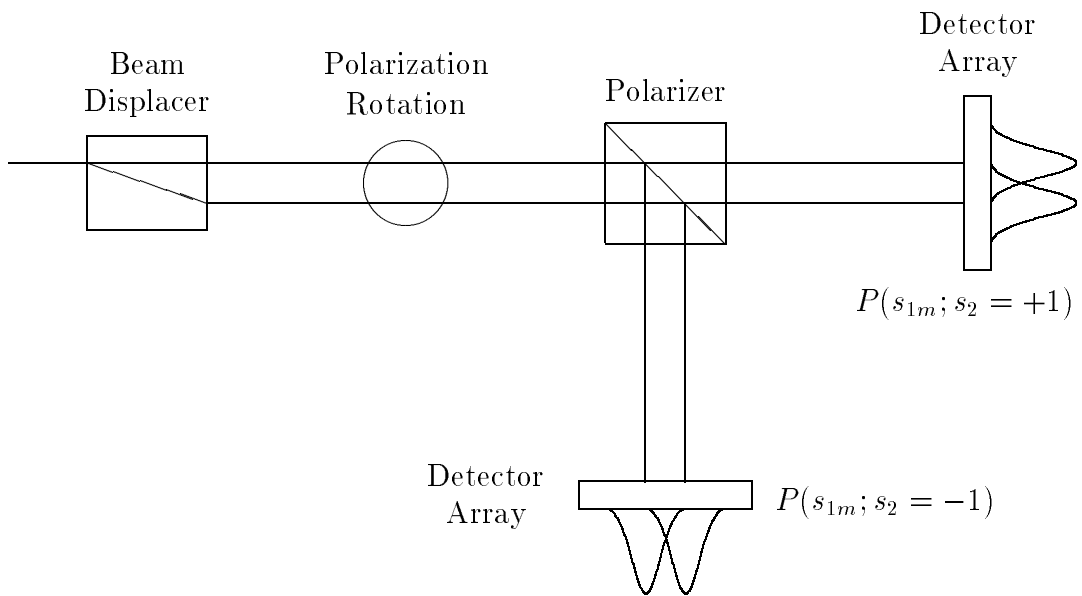


Figure 2

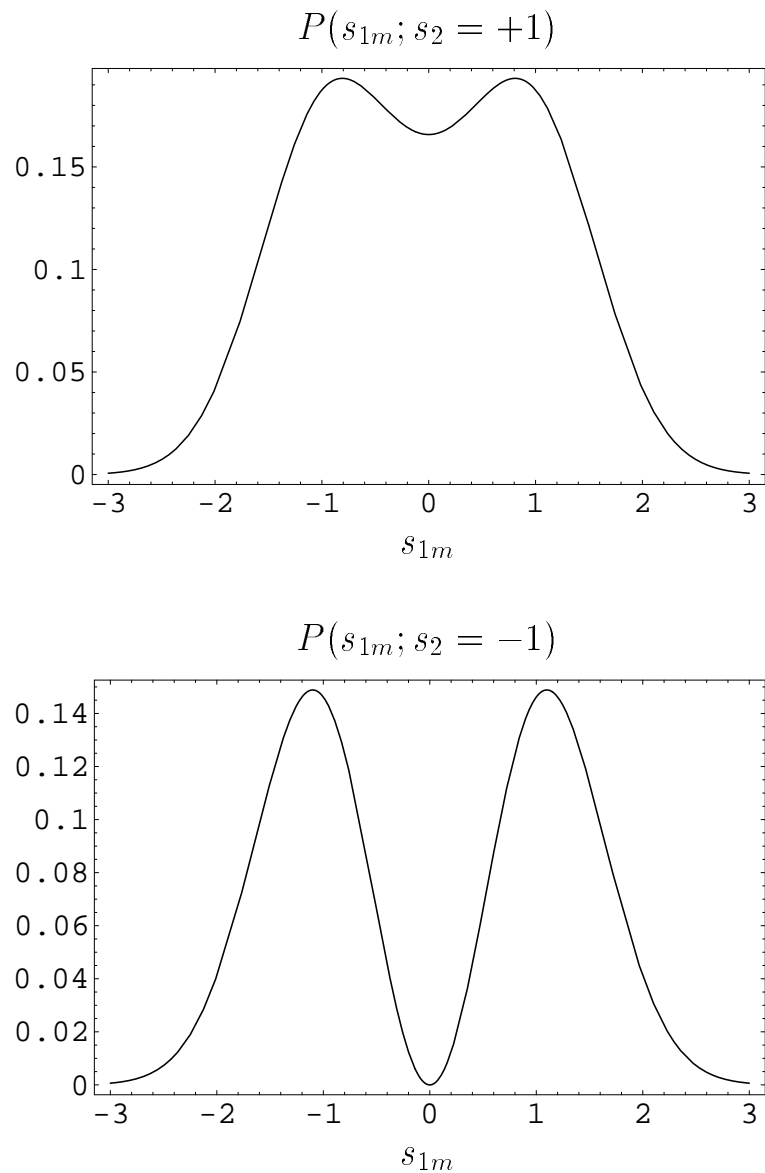


Figure 3

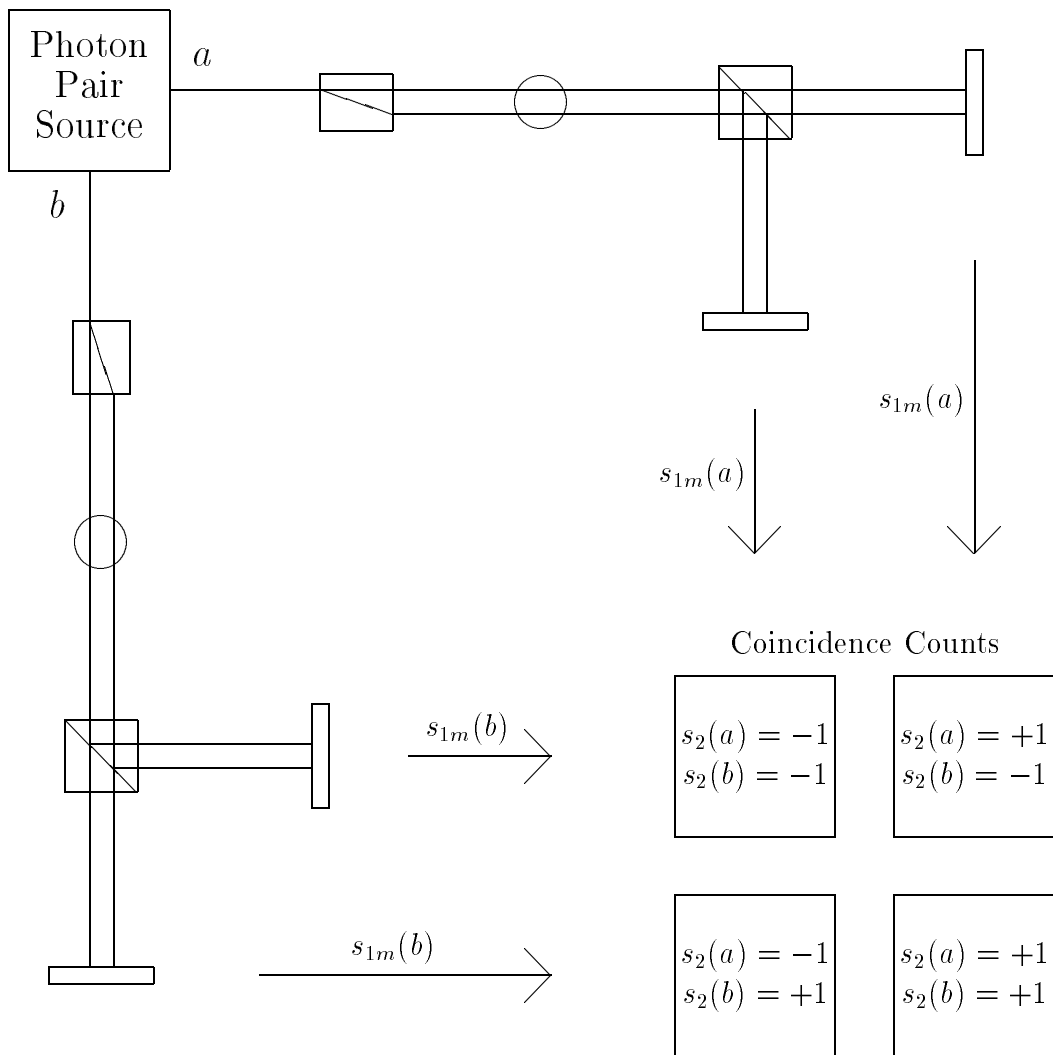


Figure 4

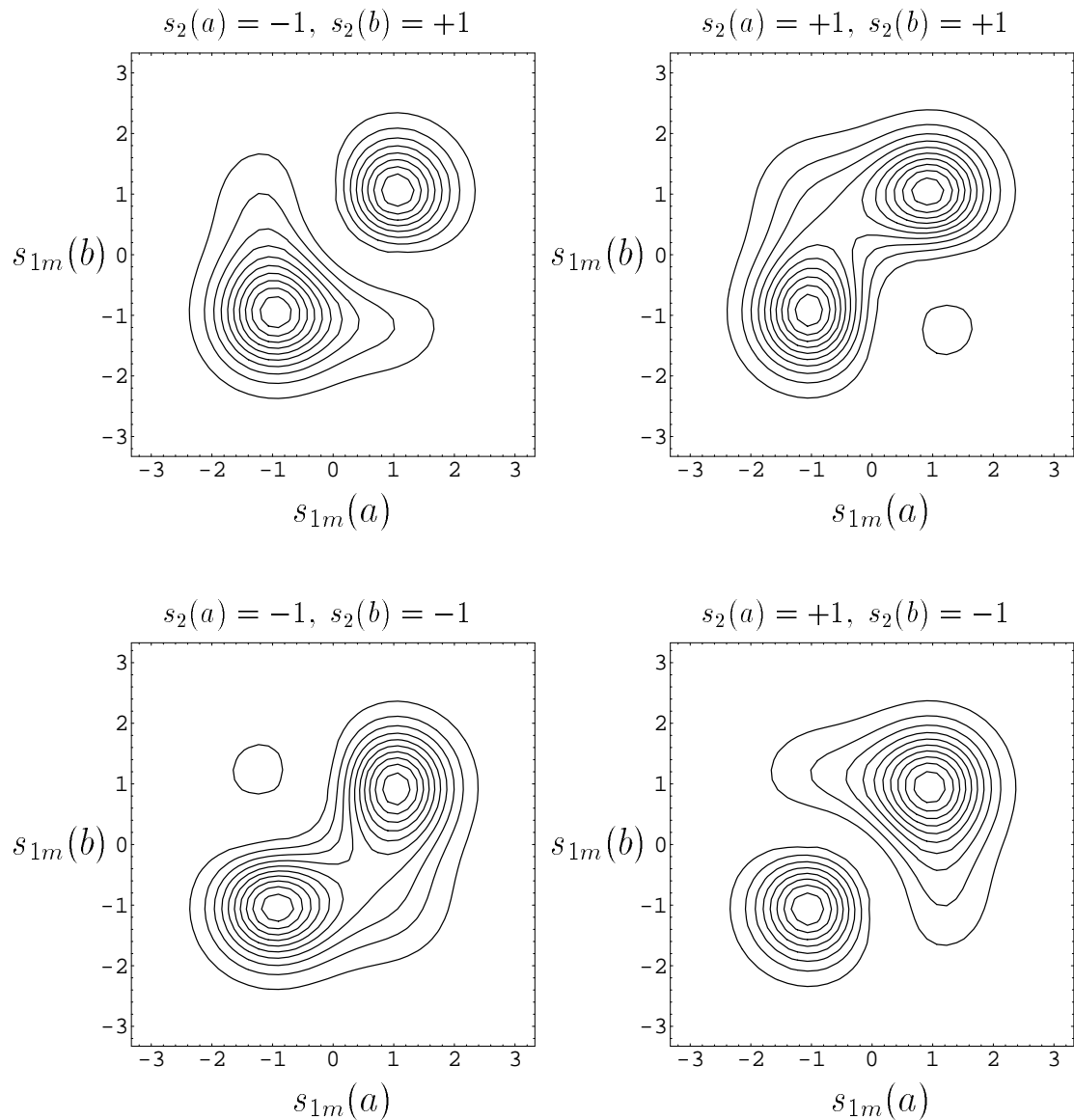


Figure 5

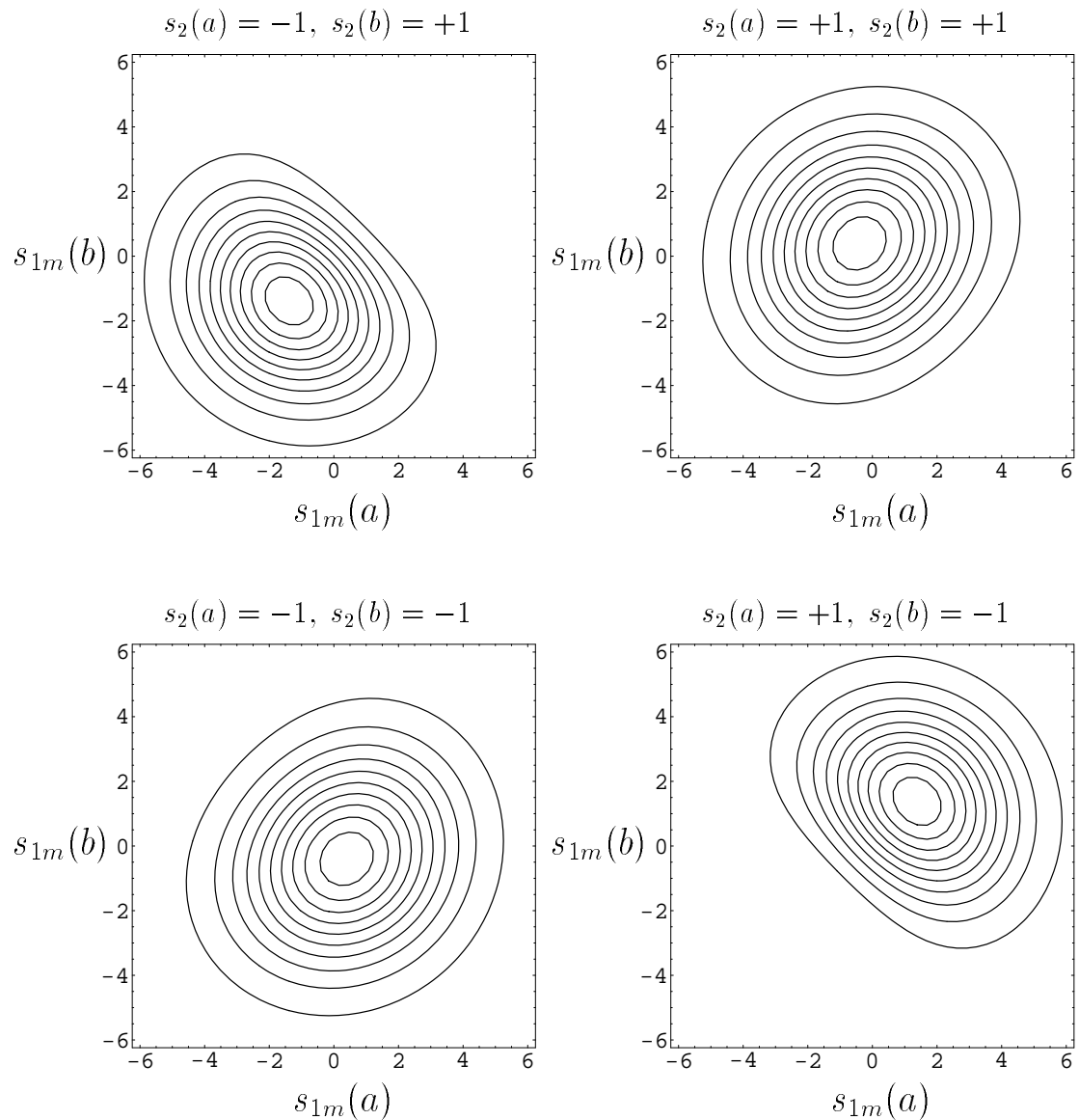


Table 1

		$(s_1(a), s_2(a))$					
$(s_1(b), s_2(b))$		$(-1, -1)$	$(0, -1)$	$(1, -1)$	$(-1, 1)$	$(0, 1)$	$(1, 1)$
$(1, 1)$		$\frac{\sqrt{2}-1}{16\sqrt{2}}$	$-\frac{1}{8\sqrt{2}}$	$\frac{\sqrt{2}+1}{16\sqrt{2}}$	$\frac{\sqrt{2}-1}{16\sqrt{2}}$	$\frac{1}{8\sqrt{2}}$	$\frac{\sqrt{2}+1}{16\sqrt{2}}$
$(0, 1)$		$\frac{1}{8\sqrt{2}}$	$-\frac{1}{4\sqrt{2}}$	$-\frac{1}{8\sqrt{2}}$	$\frac{1}{8\sqrt{2}}$	$\frac{1}{4\sqrt{2}}$	$-\frac{1}{8\sqrt{2}}$
$(-1, 1)$		$\frac{\sqrt{2}+1}{16\sqrt{2}}$	$\frac{1}{8\sqrt{2}}$	$\frac{\sqrt{2}-1}{16\sqrt{2}}$	$\frac{\sqrt{2}+1}{16\sqrt{2}}$	$-\frac{1}{8\sqrt{2}}$	$\frac{\sqrt{2}-1}{16\sqrt{2}}$
$(1, -1)$		$\frac{\sqrt{2}-1}{16\sqrt{2}}$	$-\frac{1}{8\sqrt{2}}$	$\frac{\sqrt{2}+1}{16\sqrt{2}}$	$\frac{\sqrt{2}-1}{16\sqrt{2}}$	$\frac{1}{8\sqrt{2}}$	$\frac{\sqrt{2}+1}{16\sqrt{2}}$
$(0, -1)$		$-\frac{1}{8\sqrt{2}}$	$\frac{1}{4\sqrt{2}}$	$\frac{1}{8\sqrt{2}}$	$-\frac{1}{8\sqrt{2}}$	$-\frac{1}{4\sqrt{2}}$	$\frac{1}{8\sqrt{2}}$
$(-1, -1)$		$\frac{\sqrt{2}+1}{16\sqrt{2}}$	$\frac{1}{8\sqrt{2}}$	$\frac{\sqrt{2}-1}{16\sqrt{2}}$	$\frac{\sqrt{2}+1}{16\sqrt{2}}$	$-\frac{1}{8\sqrt{2}}$	$\frac{\sqrt{2}-1}{16\sqrt{2}}$